

# UC Berkeley

## UC Berkeley Previously Published Works

### Title

Assessment of the stromal contribution to Sonic Hedgehog-dependent pancreatic adenocarcinoma.

### Permalink

<https://escholarship.org/uc/item/36d7j30b>

### Journal

Molecular Oncology, 7(6)

### Authors

Damhofer, Helene  
Medema, Jan  
Veenstra, Veronique  
et al.

### Publication Date

2013-12-01

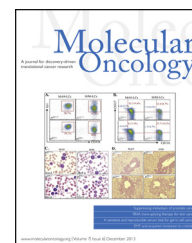
### DOI

10.1016/j.molonc.2013.08.004

Peer reviewed

available at [www.sciencedirect.com](http://www.sciencedirect.com)

ScienceDirect

[www.elsevier.com/locate/molonc](http://www.elsevier.com/locate/molonc)

## Assessment of the stromal contribution to Sonic Hedgehog-dependent pancreatic adenocarcinoma

Helene Damhofer<sup>a</sup>, Jan Paul Medema<sup>a</sup>, Veronique L. Veenstra<sup>a</sup>,  
Liviu Badea<sup>b</sup>, Irinel Popescu<sup>c</sup>, Henk Roelink<sup>d</sup>, Maarten F. Bijlsma<sup>a,d,\*</sup>

<sup>a</sup>Laboratory for Experimental Oncology and Radiobiology, Academic Medical Center, University of Amsterdam, Meibergdreef 9, 1105AZ Amsterdam, The Netherlands

<sup>b</sup>National Institute for Research and Development in Informatics (ICI), 8-10 Aversescu Boulevard, Bucharest, Romania

<sup>c</sup>Department of General Surgery and Liver Transplantation, Fundeni Clinical Institute, Bucharest, Romania

<sup>d</sup>Department of Molecular and Cell Biology, University of California, 16 Barker Hall, 3204, Berkeley, CA 94720, USA

### ARTICLE INFO

#### Article history:

Received 17 July 2013

Accepted 8 August 2013

Available online 16 August 2013

#### Keywords:

Hedgehog

Pancreatic cancer

Development

Stroma

mRNA-Seq

### ABSTRACT

Pancreatic ductal adenocarcinoma (PDAC) remains one of the most lethal malignancies. It is typically detected at an advanced stage, at which the therapeutic options are very limited. One remarkable feature of PDAC that contributes to its resilience to treatment is the extreme stromal activation seen in these tumors. Often, the vast majority of tumor bulk consists of non-tumor cells that together provide a tumor-promoting environment. One of the signals that maintains and activates the stroma is the developmental protein Sonic Hedgehog (SHH). As the disease progresses, tumor cells produce increasing amounts of SHH, which activates the surrounding stroma to aid in tumor progression. To better understand this response and identify targets for inhibition, we aimed to elucidate the proteins that mediate the SHH-driven stromal response in PDAC. For this a novel mixed-species coculture model was set up in which the cancer cells are human, and the stroma is modeled by mouse fibroblasts. In conjunction with next-generation sequencing we were able to use the sequence difference between these species to genetically distinguish between the epithelial and stromal responses to SHH. The stromal SHH-dependent genes from this analysis were validated and their relevance for human disease was subsequently determined in two independent patient cohorts. In non-microdissected tissue from PDAC patients, in which a large amount of stroma is present, the targets were confirmed to associate with tumor stroma versus normal pancreatic tissue. Patient survival analysis and immunohistochemistry identified CDA, EDIL3, ITGB4, PLAUR and SPOCK1 as SHH-dependent stromal factors that are associated with poor prognosis in PDAC patients. Summarizing, the presented data provide insight into the role of the activated stroma in PDAC, and how SHH acts to mediate this response. In addition, the study has yielded several candidates that are interesting therapeutic targets for a disease for which treatment options are still inadequate.

© 2013 Federation of European Biochemical Societies.

Published by Elsevier B.V. All rights reserved.

**Abbreviations:** CDA, cysteine deaminase; EDIL3, EGF-like repeats and discoidin I-like domains 3; GSEA, gene set enrichment analysis; HH, Hedgehog; ITGB4, integrin beta 4; PDAC, pancreatic ductal adenocarcinoma; PLAUR, plasminogen activator, urokinase receptor; SHH, Sonic Hedgehog; SPOCK1, Sparc/Osteonectin, Cwcv And Kazal-Like Domains Proteoglycan.

\* Corresponding author. Laboratory for Experimental Oncology and Radiobiology, Academic Medical Center, University of Amsterdam, Meibergdreef 9, 1105AZ Amsterdam, The Netherlands. Tel.: +31 20 5664824.

E-mail addresses: [h.damhofer@amc.uva.nl](mailto:h.damhofer@amc.uva.nl) (H. Damhofer), [j.p.medema@amc.uva.nl](mailto:j.p.medema@amc.uva.nl) (J.P. Medema), [v.l.veenstra@amc.uva.nl](mailto:v.l.veenstra@amc.uva.nl) (V.L. Veenstra), [badea@ici.ro](mailto:badea@ici.ro) (I. Badea), [roelink@berkeley.edu](mailto:roelink@berkeley.edu) (H. Roelink), [m.f.bijlsma@amc.uva.nl](mailto:m.f.bijlsma@amc.uva.nl) (M.F. Bijlsma).

1574-7891/\$ – see front matter © 2013 Federation of European Biochemical Societies. Published by Elsevier B.V. All rights reserved.

<http://dx.doi.org/10.1016/j.molonc.2013.08.004>

## 1. Introduction

Pancreatic ductal adenocarcinoma (PDAC) is one of the most challenging cancers to treat as it often remains undetected until the disease is at an advanced, essentially incurable stage. Treatment options are typically limited and prognosis is poor (Vincent et al., 2011). Although the signaling pathways and genetic aberrations in tumor cells that sustain these cells have been extensively studied, these findings have not translated into more effective therapeutic approaches for pancreatic cancer patients. Gemcitabine-based chemotherapy remains the standard of care, but offers only a marginal survival benefit measured in weeks (Burris et al., 1997).

One of the histological hallmarks of pancreatic cancer is a dense fibrotic stromal matrix (desmoplasia) composed of extracellular matrix (ECM), activated fibroblasts, inflammatory cells, as well as blood and lymphatic vessels that together can comprise the bulk (up to 90%) of the tumor volume. This stroma creates a microenvironment that supports cancer initiation, progression, metastasis formation, and drug resistance (Erkan et al., 2012). Historically, attention has been directed to the epithelial compartment of the tumor, but the recent recognition of the stroma-mediated support for the tumor suggests that the stroma could be an attractive target for new treatment modalities. The mechanisms behind this support, however, are still poorly understood. Several factors have been implied to mediate the interaction between these two compartments with transforming growth factor-beta (TGF- $\beta$ ), platelet derived growth factor (PDGF) and Sonic hedgehog (SHH) signaling being the more prominently studied pathways (Mahadevan and Von Hoff, 2007).

The SHH pathway is best known for its many roles in development. In model systems ranging from frog, fish, mouse, to fruit flies the SHH pathway has been shown to provide spatio-temporal information to cells in many developing organs and tissues (Bijlsma et al., 2004). In adult organisms, the pathway has been shown to regulate gastrointestinal tissue homeostasis, and the maintenance of certain stem cell populations, but in addition to its role in development and tissue homeostasis, SHH pathway activation has been shown to cause and sustain cancer growth (Teglund and Toftgard, 2010).

Excessive production of SHH ligand is a causal event in many tumors of the upper gastrointestinal tract (Berman et al., 2003; Thayer et al., 2003). SHH has been shown to be a critical mediator of pancreatic cancer initiation, progression, angiogenesis and metastasis, and several SHH response pathway inhibitors are currently being tested in pancreatic cancer patients (Thayer et al., 2003). Remarkably, cells of epithelial origin in SHH-dependent tumors are quite resistant to small molecule inhibitors of Smo that are highly effective in cell-based models (Yauch et al., 2008). This observation, combined with the finding that SHH-induced tumors often contain large numbers of stromal cells, has led to the idea that the stromal cells and epithelial cells are mutually dependent. SHH derived from the epithelial cells is a prime candidate to mediate growth of the stroma, which in turn support the epithelial cells in an unknown manner (Bailey et al., 2008). This reciprocal *modus operandi* of SHH in PDAC may be the cause of the disappointing clinical efficacy observed in these

tumors using HH pathway inhibitors with proven *in vitro* efficiency. Here we try to identify the SHH-dependent factors that mediate the crosstalk between epithelial and stromal cells. This will aid in the development of targeted, stromal-directed therapies that reduce desmoplasia and the tumor-promoting properties of this compartment.

To identify the proteins that mediate SHH-dependent tumor-stroma crosstalk, we employed a 3D coculture system to mimic the stromal–epithelial interaction *in vitro*. This mixed species model in combination with next generation sequencing allowed us to dissect and distinguish the signals derived from either compartment and lead us to the identification of several extracellular factors produced by stromal cells in response to Hh pathway activation. We show as well that expression of some of these factors is associated with poor clinical outcome and therefore present interesting targets for further investigation.

## 2. Materials and methods

### 2.1. Cell culture and transfections

HS766T, BxPC3, MIA PaCa-2, PANC-1, 10.7, DLD-1, C3H10T1/2 (ATCC, Manassas, VA) and Capan-2 cells (Cell Line Service, Eppelheim, Germany) were cultured in DMEM (Cambrex, East Rutherford, NJ) containing 10% fetal calf serum (FCS (Cambrex)) according to routine cell culture procedures. Shh-LIGHT II cells (Taipale et al., 2000), ATCC) were grown in the abovementioned medium supplemented with neomycin (400  $\mu$ g/mL) and zeocin (150  $\mu$ g/mL).

Transfections were performed using Effectene (Qiagen, Germany) according to manufacturer's directions. For reporter assays, cells were transfected in 12-well cell culture plates. Per well, 1  $\mu$ g DNA was used. For other transfections, cells were transfected in 6-well plates (2  $\mu$ g DNA per well).

### 2.2. Coculture model

To mimic the 3-dimensional organization of tumor/stromal interaction, we cultured tumor cell lines with fibroblasts 1:1 on non-adherent (hydrophobic) 60  $\times$  15 mm dishes (Greiner) in DMEM with 0.5% FCS, on a rotary shaker at 55 rpm. Under these conditions the tumor cells and the fibroblasts form mixed aggregates. The aggregates were cultured for 5 d prior to further analysis.

### 2.3. RT-PCR and quantitative real-time RT-PCR

Mia PaCa-2 cocultures were lysed in Trizol (Invitrogen) and RNA was isolated according to the manufacturer's protocol. cDNA was synthesized using Superscript II (Invitrogen) and random primers (Invitrogen). PCR was performed on a BioRad MJ Mini thermocycler and product was analyzed by agarose gel electrophoresis. Total RNA from Capan-2 cocultures was isolated using RNeasy Mini Kit (Quiagen, Germany) and 1  $\mu$ g RNA was used for cDNA synthesis using Superscript III (Invitrogen) according to manufacturer's instructions. Real-time quantitative RT-PCR was performed with SYBR green (Roche) on the LC480

II (Roche). Relative expression of genes was calculated using the comparative threshold cycle (CT) method and values were normalized against that of housekeeping gene *hGAPDH/mGapdh* for human and mouse respectively. Species-specific primer sequences are listed in [Supplementary Table 3](#).

#### 2.4. Reporter assay

Cocultures with the Shh-LIGHT II stably transfected reporter fibroblasts were grown and after 5 d, lysed with passive lysis buffer as provided by Promega and luciferase activity was assayed according to the Promega Dual-Glo Luciferase Assay System (Promega) protocol on a Victor plate reader (PerkinElmer, Waltham, MA). Each Firefly luciferase value was corrected for its CMV-driven Renilla luciferase standard to correct for nonspecific effects.

#### 2.5. Preparation of RNA-Seq libraries

RNA from cocultures from 3 separate experiments was isolated, efficient 5E1 treatment confirmed by RT-PCR for *mPtch1*, and libraries were constructed using the mRNA-Seq Sample Preparation Kit (Illumina, Hayward, CA) according to manufacturer's protocol. Sequencing runs were performed on an Illumina 1G Genome Analyzer. Reads were non-paired end, 31 bp, and mapped and annotated to the human as well as the mouse genome using ArrayStar 3.0 software (DNASTar, Madison, WI) with the Qseq module. The human orthologs of mouse genes were downloaded from MGI (<http://www.informatics.jax.org/>) and Gene Ontology analysis using the GO cellular component term 'extracellular region' was performed.

#### 2.6. SHH knockdown cell lines

Lentiviral particles were produced by transiently transfecting HEK293T cells with pLKO construct targeting SHH (see [Supplemental Table 4](#)) or a scrambled non-targeting control shRNA (shc002, Sigma) and the packaging plasmids pMD2.G and psPAX2 using Fugene HD (Roche). 48 h and 72 h after transfection the supernatant was harvested, filtered through a 0.45 µm filter (Millipore, Germany) and subsequently used to transduce 60% confluent Capan-2 cells in the presence of 5 µg/ml polybrene (Sigma) overnight. Two days after transduction cells were selected for stable expression of shRNA with 2 µg/ml puromycin (Sigma) and knockdown efficiency was analyzed by qRT-PCR.

#### 2.7. Gene set enrichment analysis

Gene set enrichment analysis (GSEA, v2.10) software was downloaded from the Broad Institute (<http://www.broadinstitute.org/gsea>) and used for analysis according to the author's guidelines ([Subramanian et al., 2005](#)). Briefly, genes are ranked according to their association with a given phenotype (expression in tumor tissue relative to normal pancreas). Genes at the top of the rank associate positively with the phenotype tumor while genes at the bottom of the rank associate negatively. GSEA was performed to determine whether the extracellular genes found 2-fold down-regulated in response to 5E1 treatment are enriched within PDAC tumor samples compared to

normal pancreatic tissue in publicly available datasets (GSE15471 and GSE16515). 1000 phenotype permutations were used to determine significance of the enrichment score. An area-proportional Venn diagram to display the overlap of genes found enriched in both datasets was generated using the BioVenn online tool ([Hulsen et al., 2008](#)).

#### 2.8. Survival and statistical analysis

Overall survival (OS) was defined as the interval between the date of surgery and death of each patient ( $n = 35$ ). Patients alive at the last follow-up were censored. For single-gene survival prediction, the median expression value of each gene was used as a cutoff to generate two groups of patients having either a low or high relative expression. Survival curves were constructed using Kaplan–Meier analysis and  $p$  values were calculated using the log-rank test in SPSS 19.0 (SPSS, Inc.). Other statistical procedures were carried out using GraphPad Prism 5. All values were presented as mean  $\pm$  SEM. A value of  $p < 0.05$  was considered to be statistically significant.

#### 2.9. Immunohistochemistry

Resected tumors from patients were fixed in 4% formalin prior to paraffin embedding. Sections of 5 µm were prepared on a microtome. Tissue sections were deparaffinized and antigen retrieval was performed using 10 mM sodium citrate solution and boiling for 15 min. Endogenous peroxidase activity was blocked with 3% hydrogen peroxide in PBS. Aspecific staining was blocked using 5% normal goat serum for 20 min at room temperature. The primary antibodies were diluted in normal antibody diluent (KliniPath), applied on tissue sections and incubated overnight at 4 °C in a humidified chamber. For amplification of the staining Brightvision + post antibody block (Immunologic) was used prior to the addition of the secondary antibody, poly-HRP-anti Ms/Rt/Rb IgG (Immunologic) both for 30 min at room temperature. Visualization of stainings was performed with vector novaRED peroxidase (Vector) according to manufacturer's protocol, counterstained with 30% haematoxylin and mounted tissue sections with non-aqueous medium. Antibodies used for immunohistochemistry were: anti-CDA, C-terminal (Abcam, ab82346); anti-EDIL3 (Abcam, ab151308); anti-SPOCK1 (Sigma, HPA007450). All were used at 1:200 dilution. The specimens were collected in the Academic Medical Center in compliance with the Declaration of Helsinki for experiments performed on humans and the institute's ethical committee.

---

### 3. Results

#### 3.1. Epithelial tumor cells and fibroblasts show mutual growth support in a 3-D coculture model

We designed an experimental model to study the signaling that sustains mutually dependent growth support between the epithelial- and stromal compartments, and thus mimic the strong relationship between stroma and epithelium found in pancreatic adenocarcinoma. To this end, human pancreatic tumor cell lines were cocultured together with mesenchymal

fibroblasts under non-adherent, low-serum conditions. C3H10T1/2 fibroblasts were chosen to model the stroma for this study, as these are highly responsive to Hedgehog (HH) ligands.

When culturing these fibroblasts under embryoid body-like culture conditions for five days, hardly any cells survived, and they did not assemble into aggregates (Figure 1A). In contrast, PANC-1 pancreatic adenocarcinoma cells formed small spheres when cultured under identical conditions, indicating that pancreatic tumor cells were able to sustain some degree of viability (Figure 1B). Mixing the two cell types resulted in aggregates that were significantly larger (Figure 1C, quantification of cell number in Figure 1D), suggesting that these two cell types exchange factors to provide growth or survival support when grown in contact.

Several pancreatic adenocarcinoma cell lines were subsequently tested in this coculture model. As a control, cancer cells were grown in monoculture at an identical starting density to the cocultures. All cell lines tested showed increased cell numbers (Figure 1E, indicated as fold expansion of cancer cell fraction relative to input) when cocultured with fibroblasts, indicating that these support the growth of the adenocarcinoma cells. Although only a small fraction of the cocultures was found to be of fibroblast origin (Figure 1F), this minor fraction appeared to mediate a strong growth-stimulatory effect on the tumor cells. Given the close proximity between the fibroblast and adenocarcinoma cells within these cocultures, the mutual support observed could very well be mediated by signals that only act at a short range, and which would not be able to signal in different coculture setups or medium transfer experiments. One of such range-limited signals is SHH, the

expression of which is strongly involved in the induction of PDAC.

### 3.2. SHH produced in pancreatic adenocarcinoma cells signals efficiently to fibroblasts in non-adherent cocultures

The PDAC cell lines tested above share that they have been reported to have high levels of HH (HH; all three Hedgehog ligand homologs) expression, and this HH is reported to signal to the stroma to aid in the tumor cells' survival and growth (Berman et al., 2003; Yauch et al., 2008). To assess the signaling potency of the HH ligands produced in the adenocarcinoma cells, PDAC cells were cocultured with fibroblasts stably transfected with a HH-pathway reporter (Shh-LIGHT II (Taipale et al., 2000)) to allow the quantification of the levels of HH pathway activation *in trans* (Figure 2A). To selectively prevent HH signaling, 5E1 blocking antibody was used (Ericson et al., 1996). All the PDAC cell lines tested activated the Hh pathway in the reporter cells, and this activation was inhibited by 5E1, showing that it is a HH-dependent effect. In fact, the HH from the PDAC cells induced a stronger HH response in the reporter cells than purmorphamine, a small molecule Smo activator (Sinha and Chen, 2006). Although the colon cancer cell line DLD-1 induced some pathway activity in the fibroblasts, this activation could not be diminished by 5E1. This demonstrates it to be HH-independent, which is consistent with these tumors not being HH-driven or -producing.

To assess the biological activity of PDAC cell line-derived HH in another experimental system, a mouse embryonic stem (ES) cell model for motor neuron differentiation was

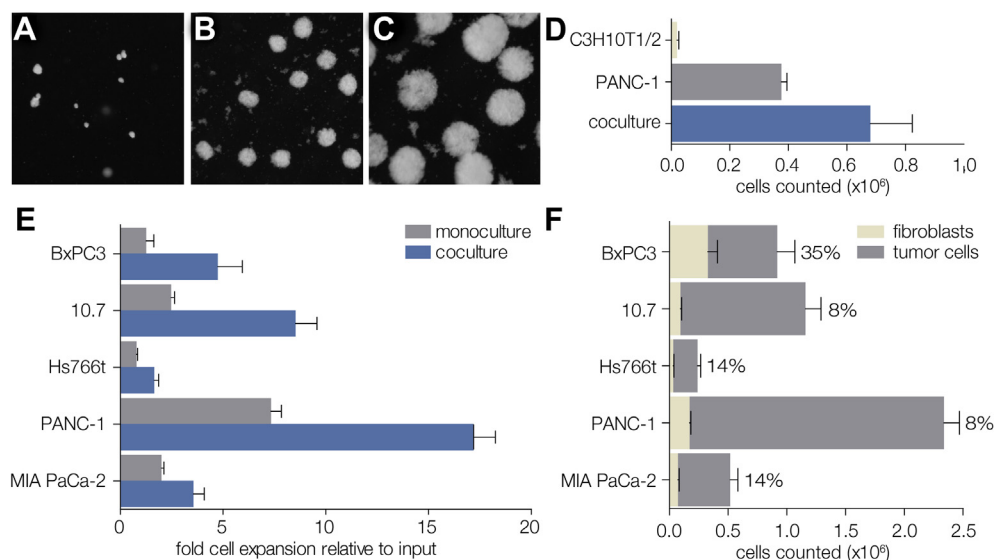


**Figure 1 – Tumor cells and fibroblasts show mutual growth support in non-adherent cocultures.** A,  $2.5 \times 10^5$  C3H10T1/2 fibroblasts were seeded under the non-adherent conditions described in the Materials and Methods section. After 5 d, dark field micrographs were taken on a Zeiss Lumar V12 microscope. B, as for panel A, using  $2.5 \times 10^5$  PANC-1 cells. C, as for panel A, using equal amounts of C3H10T1/2 and PANC-1 cells to a total of  $2.5 \times 10^5$  cells. D, cells as indicated on y-axis were grown in monoculture or together with C3H10T1/2 cells, both conditions at a total cell count of  $2.5 \times 10^5$ . After 5 d, cells were trypsinized, resuspended and counted.  $n \geq 4$ , shown is mean  $\pm$  SEM. E, fibroblasts were labeled with Cell Tracker Green and cocultured with the pancreatic tumor cell lines indicated on y-axis. After 5 d, cocultures were dissociated and fluorescent cells were counted to determine fraction of fibroblasts per coculture. Plotted on the x-axis is the fold expansion of cancer cells relative to the initial cell input.  $n = 4$ . F, showing the raw cell counts, and fraction of fibroblasts and cancer cells from experiment in panel E.

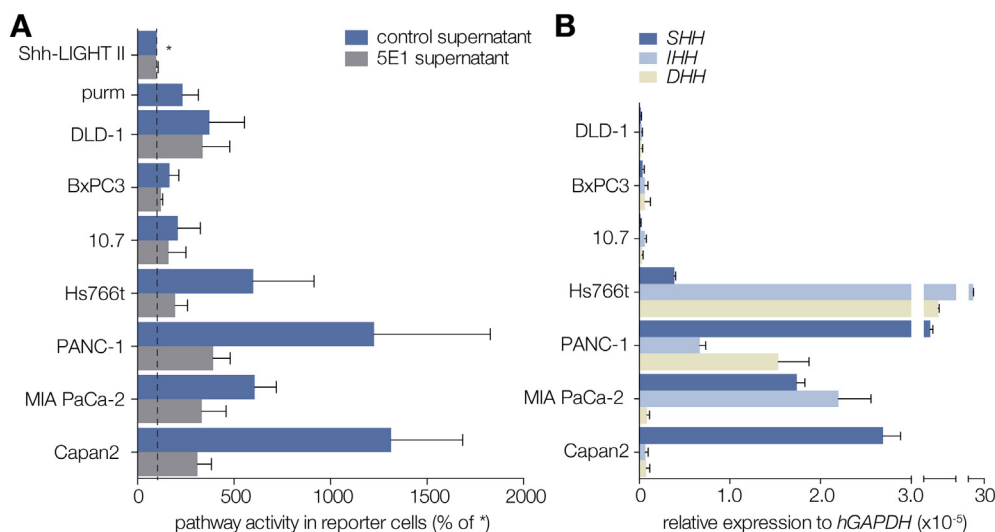


**Figure 2** – Shh produced in pancreatic adenocarcinoma cells signals to fibroblasts in non-adherent cocultures. **A**, indicated cell lines (*y*-axis) were cocultured under non-adherent conditions in the presence of either control supernatant, or five-fold diluted 5E1 Shh blocking antibody (0.02  $\mu\text{g}/\text{mL}$ ). In addition, a Shh-LIGHT II monoculture was stimulated with Hh pathway agonist 10  $\mu\text{M}$  purmorphamine. After 5 d, cocultures were harvested and pathway activity in Shh-LIGHT II cells was measured. Shown is the percentage of pathway activity compared to control treated Shh-LIGHT II monoculture, indicated by asterisk.  $n \geq 4$ , shown is the mean  $\pm$  SEM. **B**, qRT-PCR analysis for *bSHH*, *bIHH*, *bDHH* transcripts in a panel of pancreatic adenocarcinoma cells and the DLD-1 colon cancer cell line. Expression is shown relative the reference gene *hGAPDH* ( $2^{-\Delta\text{Ct}}$ ),  $n = 3$ , mean  $\pm$  SEM.

chosen. Motor neuron induction requires HH pathway activation, and can be assessed by the expression of HB9, a motor neuron-specific protein (Wichterle et al., 2002). When *HB9::GFP* (HBG) ES cells, which express GFP under the control of the HB9 promoter, were grown as EBs together with MIA PaCa-2 cells, robust GFP expression was observed (Figure S1). This confirms that also in a developmental model, PDAC tumor cell-derived SHH is a potent transsignaling molecule.

To formally confirm the production of HH ligands in the cancer cells tested and to identify which homologs are involved, quantitative real-time RT-PCR analysis was performed to measure HH transcript levels in these cell lines (Figure 2B). As expected, the PDAC cell lines tested had considerable amounts of HH ligand mRNA, reflecting their capacity to activate the pathway in Shh-LIGHT II cells. The MIA PaCa-2 cell line was used for further analyses, as this cell line showed high HH expression and strong trans-signaling capacity.

### 3.3. Next generation sequencing reveals reciprocal signaling between tumor and stromal cells

In order to identify the stroma-generated factors in response to HH pathway activation, a transcriptome-wide quantitative sequencing of MIA PaCa-2/C3H10T1/2 aggregates in the absence and presence of the blocking antibody 5E1 was performed. The use of cocultures prior to transcriptome sequencing rather than the addition of SHH ligand to fibroblast monocultures was chosen because it is plausible that some genes rely on both HH ligand as well as other tumor-derived signals. The mouse and human transcriptome are sufficiently different in sequence to allow for unambiguously discrimination of changes in gene expression in both the mouse fibroblasts and human MIA PaCa-2 cells. Cocultures

were treated with control or 5E1 antibody and after RNA isolation, RT-PCR for mouse *Ptch1* was performed in order to confirm activation of the HH pathway in the cocultured fibroblasts compared to adherent fibroblast monoculture. The addition of 5E1 antibody to the cocultures was able to strongly diminish the expression of *Ptch1* in the mouse fibroblasts, which confirmed that the observed *Ptch1* induction is a specific HH effect (Figure 3B). Three cocultures were verified for *Ptch1* repression in response to 5E1, and used for further analysis.

For transcriptome sequencing, mRNA was isolated from total RNA as used for the RT-PCR and libraries were constructed for sequencing on the Illumina Genome Analyzer (Figure 3A) (Mortazavi et al., 2008). For the cocultures, approximately  $17 \times 10^6$  reads were generated, of which half could be successfully mapped to either the mouse or human genome. Of these reads, approximately 5% were mapped on the mouse genome, consistent with the relative contribution of the mouse fibroblasts to the coculture aggregates (Figure 1F). Average fold changes between control antibody and 5E1 treated cocultures of 3 experiments was calculated, and a scatterplot of these values is shown in Figure 3C.

To identify HH-dependent stromal derived proteins that signal to the tumor compartment rather than the proteins that are involved in stroma activation, mouse genes were selected that were at least 2-fold reduced in response to 5E1 treatment. This approach yielded approximately 2200 genes (Supplementary Table 1). To identify potential reciprocal signals, i.e. proteins that are induced by HH and are able to signal back to the tumor cells from the stroma, these 2200 genes were filtered using gene ontology for extracellular proteins. This yielded 249 genes that were considered for further analysis (workflow of analysis show in Figure 4A).

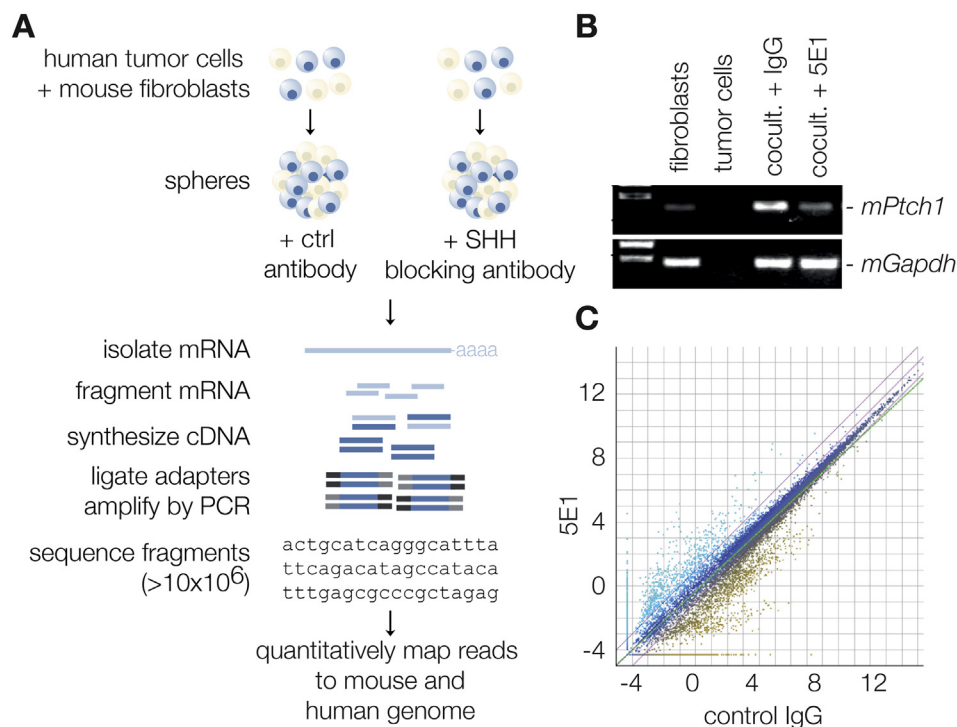


**Figure 3** – Experimental setup for mRNA-Seq analysis of non-adherent cocultures. **A**, diagram describing the workflow of the experiment. **B**, RT-PCR analysis for *mPtc1* and *mGapdh* on C3H10T1/2 and MIA PaCa-2 mono- and cocultures treated with control (IgG) or 5E1 antibody supernatant (0.02  $\mu\text{g}/\text{mL}$ ). Cells were cultured for 5 d, and antibody was added during the last 24 h. RNA was isolated and RT-PCR was performed. **C**, scatterplot showing fold changes in mouse gene expression following 5E1 treatment of cocultures as determined by mRNA-Seq analysis. Purple lines indicate 2-fold changes.

### 3.4. Hedgehog dependent stromal genes are overexpressed in pancreatic cancer tissue

To select genes that are associated with human disease, gene set enrichment analysis (GSEA) was employed with the 249 extracellular SHH-dependent gene set on a publically available whole-tissue microarray dataset of pancreatic cancer patients that contained normal pancreatic tissue counterparts (Badea et al., 2008). This allowed ranking of the genes according to their differential expression between tumor and adjacent normal pancreas. The extracellular gene set showed a good enrichment score and was significantly associated with tumor compared to the normal pancreatic tissue (Figure 4B), suggesting that the majority of the identified extracellular factors was indeed over-expressed in cancer tissue. The grey shaded area in the enrichment plot represents the genes that most strongly associate with tumor tissue, also called 'leading edge' genes.

To confirm the degree of tumor association of these genes in an independent dataset, a second whole-tissue microarray pancreatic cancer set was used for GSEA with the extracellular SHH-dependent gene list (Pei et al., 2009). Again, many of the extracellular candidate genes were found to be enriched in the tumor samples compared to normal tissue, although the overall enrichment did not reach statistical significance (Figure 4C). A remarkable congruence was found in the leading edge genes of both datasets, and the 35 overlapping genes (Figure 4D) that displayed strongest differential expression

between tumor and normal tissue in both datasets (leading edge gene list) were now considered relevant HH-dependent stromal target genes in PDAC (summarized in Table 1), and used for further validation.

A previously reported study that showed the stroma to mediate the tumor promoting effect of SHH in PDAC provided expression data from HH antagonist-treated PDAC xenografts (Yauch et al., 2008). Samples from these experiments were hybridized to human and mouse chips and for species specificity, this method thus relies on hybridization stringency. When we tested the targets from our 35 gene list in these microarray data, we found 6 genes that were significantly downregulated by treatment with HH antagonist (Col8A1, Cp, Edil3, Plaur, Spock1, and Wnt2), and two genes that were in fact upregulated by this inhibitor (C1qtnf3 and Cxcl16). These data suggest a certain degree of overlap between the two experimental setups despite their obvious technical differences, and identifies genes that are robustly induced by SHH in tumor-stroma interaction models.

### 3.5. Hedgehog responsive stromal genes identified by next generation sequencing validate in vitro and associate with survival in pancreatic cancer patients

To confirm the HH-dependency of the genes derived from the GSEA analysis and to control for experimental and technical artifacts, the cocultures were repeated with some variations to the original model: First, a different pancreatic cancer cell

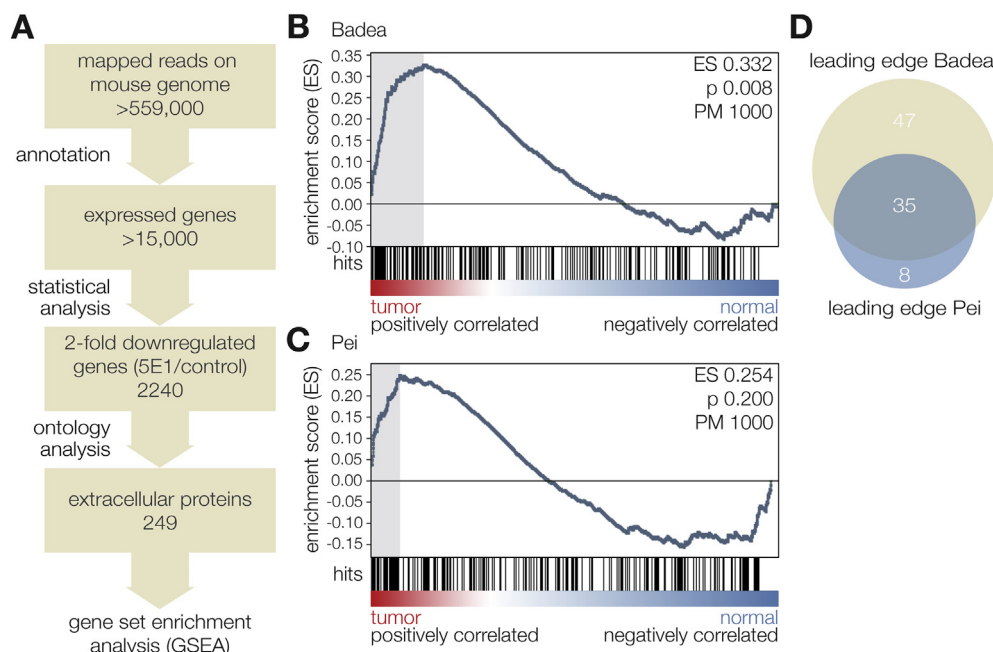


**Figure 4 – Hedgehog responsive extracellular genes are overexpressed in tissue of pancreatic cancer patients. A, workflow of data processing after transcriptome sequencing. B, gene set enrichment analysis (GSEA) using transcriptome sequencing generated extracellular HH-dependent stromal genes on a tumor/normal PDAC expression dataset by Badea et al. (GSE15471). C, GSEA on PDAC expression dataset by Pei et al. (GSE16515). ES, enrichment score; PM, phenotype permutations;  $p$ , FWER  $p$ -value. D, area-proportional Venn diagram of overlap in hedgehog responsive extracellular genes found overexpressed in both pancreatic cancer datasets.**

line to was used control for any unspecific effects caused by choosing a specific cell line rather than specific interference with HH signaling. Second, a knockdown strategy was chosen to be able to downregulate SHH more consistently in the tumor compartment. As a consequence of these first two considerations, Capan-2 cells were chosen, as they show good trans-signaling capacity (Figure 2A) and are the only cells from the tested panel to only express SHH and not IHH or DHH (Figure 2B). Third, conventional quantitative RT-PCR was used to assess the expression levels of randomly selected candidates from the next generation sequencing-generated leading edge gene set.

Knockdown of SHH in Capan-2 cells was efficient and did not result in decreased HH pathway activity in these cells (Figure S2). However, in a coculture setting, nearly all of the targets that were selected from the transcriptome sequencing were downregulated in the mouse compartment following SHH knockdown (14 out of 15; 93%; Figure 5). This shows that indeed a large number of the stromal genes are regulated by HH pathway independently of the cancer cell line used as ligand source, or the way of pathway blockage. Furthermore, this validation effort confirms the accuracy of our transcriptome sequencing effort.

Next, the expression of SHH-dependent stromal targets was correlated with the prognosis of PDAC patients. When patients were split by the median expression of the genes from the GSEA selected set, the majority of genes did not show significant differences in overall survival when tested individually in Kaplan Meier analysis (Supplementary Table 2), but we did find that patients with high TNFSF13 expression

show an increase in post-operative survival (Figure 6A). The reason for this remains elusive, as TNFSF13 is typically considered a tumor-promoting protein (Planelles et al., 2008). More interestingly, several genes were identified of which high expression significantly associated with poor prognosis (Figure 6B–F). These genes; CDA, EDIL3, ITGB4, PLAUR and SPOCK1, differ greatly in their function, but most have been described in the context of tumor biology before, albeit not necessarily in PDAC making them interesting new targets in this disease. Immunohistochemical analysis of resected patient material confirmed presence of CDA, EDIL3, and SPOCK1 in the desmoplastic stroma (Figure 6G–I), although some staining was also observed in the tumor cells. Whereas EDIL3 and SPOCK1 staining was cytoplasmatic, CDA showed mainly nuclear staining in agreement with literature (Somasekaram et al., 1999) and functionality of this enzyme in nucleoside metabolism. In the case of ITGB4, immunoreactivity was mainly found in the epithelial fraction of the tissue section, but some parts of the surrounding stroma stained positive as well (Figure S3). We were unable to observe staining for PLAUR. Functional experiments should reveal the role of the targets identified here, their importance to the progression and resistance of PDAC, and assess their suitability as therapeutic targets.

#### 4. Discussion

It has been shown that many, if not most, tumors of the upper gastrointestinal tract rely on excessive SHH expression for



**Table 1 – HH-dependent stromal target genes in PDAC derived from GSEA on two independent PDAC datasets. Fold downregulation of mRNA reads in the 5E1 treated cocultures compared to control treated cocultures is shown. Reads/kb, average reads for each gene from 3 cocultures relative to gene length in kilobase.**

Gene symbol	Gene name	CTR	5E1	Fold down mRNA-Seq	Affymetrix probe
ADAMTS6	A disintegrin-like and metalloprotease (reprolysin type) with thrombospondin type 1 motif	1.651	0.822	<b>2.01</b>	237411_at
C1QTNF3	C1q and tumor necrosis factor related protein 3	0.748	0.180	<b>4.16</b>	220988_s_at
CDA	Cytidine deaminase	13.218	5.975	<b>2.21</b>	205627_at
CDCP1	CUB domain-containing protein 1	3.231	1.327	<b>2.43</b>	218451_at
CMTM7	CKLF-like MARVEL transmembrane domain containing 7	59.329	27.647	<b>2.15</b>	226017_at
COL22A1	Collagen, type XXII, alpha 1	1.997	0.998	<b>2.00</b>	228873_at
COL8A1	Collagen, type VIII, alpha 1	10.432	5.163	<b>2.02</b>	226237_at
CP	Ceruloplasmin (ferroxidase)	34.476	3.426	<b>10.6</b>	1558034_s_at
CST6	Cystatin E/M	1.194	0.051	<b>23.4</b>	206595_at
CXCL16	Chemokine (C-X-C motif) ligand 16	12.286	3.141	<b>3.91</b>	223454_at
EDIL3	Developmental endothelial locus-1 isoform a	4.315	0.830	<b>5.20</b>	207379_at
EFNA4	Ephrin A4	27.888	11.161	<b>2.50</b>	205107_s_at
ERBB2IP	ErbB2 interacting protein isoform 2	0.918	0.286	<b>3.21</b>	217941_s_at
FCGR3A	Fc gammaRIV	2.376	0.051	<b>46.6</b>	204006_s_at
FGF1	Fibroblast growth factor 1	3.808	0.051	<b>74.7</b>	205117_at
HAPLN3	Hyaluronan and proteoglycan link protein 3	1.650	0.530	<b>3.11</b>	227262_at
HPSE	Heparanase	5.415	1.845	<b>2.93</b>	219403_s_at
IL1RN	Interleukin 1 receptor antagonist	35.028	8.857	<b>3.95</b>	212657_s_at
IL4I1	Interleukin 4 induced 1	8.558	1.884	<b>4.54</b>	230966_at
ITGB4	Integrin beta 4 isoform 2	0.275	0.051	<b>5.39</b>	204990_s_at
KLK6	Kallikrein 6 (neurosin, zyme)	39.861	5.655	<b>7.05</b>	204733_at
LAMC2	Laminin, gamma 2	23.294	10.185	<b>2.29</b>	202267_at
LCN2	Lipocalin 2	50.667	22.310	<b>2.27</b>	212531_at
MMP28	Matrix metalloproteinase 28	21.710	1.586	<b>13.7</b>	239273_s_at
NMU	Neuromedin U	1.110	0.202	<b>5.50</b>	206023_at
NRG3	Neuregulin 3	1.677	0.548	<b>3.06</b>	229233_at
NRP2	Neuropilin 2 isoform 5 precursor	0.655	0.095	<b>6.89</b>	225566_at
PLAUR	Urokinase plasminogen activator receptor	179.778	80.240	<b>2.24</b>	211924_s_at
SEMA3C	Semaphorin 3C	4.922	1.271	<b>3.87</b>	203789_s_at
SERPINA1	Serine (or cysteine) proteinase inhibitor	1.636	0.572	<b>2.86</b>	202833_s_at
SPOCK1	Sparc/osteonectin, cwcv and kazal-like domains proteoglycan (testican) 1	0.129	0.051	<b>2.53</b>	202363_at
TGFA	Transforming growth factor alpha	0.176	0.051	<b>3.45</b>	205016_at
TNFSF11	Tumor necrosis factor (ligand) superfamily, member 11	0.457	0.223	<b>2.05</b>	210643_at
TNFSF13	Tumor necrosis factor (ligand) superfamily, member 13	6.406	0.473	<b>13.5</b>	210314_x_at
WNT2	Wingless-related MMTV integrationsite 2	0.158	0.051	<b>3.10</b>	205648_at

their progression. Because of the high mortality rates associated with these malignancies, the biology behind these tumors has been the subject of an intense research effort. Unfortunately, the epithelial cells in these SHH-producing cancers have turned out to be remarkably resistant to SHH pathway inhibitors. In addition, data suggest that the stromal compartment in tumors can also adapt to chronic HH pathway inhibition (Neesse et al., 2011; Olive et al., 2009). It would probably be preferable to target additional SHH-dependent mediators of tumor progression besides SMO and for this, we need to better understand the molecules involved in the HH-mediated crosstalk between tumor and surrounding stromal cells.

For the present study, a model to mimic this epithelial–stromal interaction *in vitro* was set up, by growing chimeric aggregates, made up of a murine stromal HH responsive compartment, and a human tumor epithelial compartment expressing HH ligands. By using next-generation sequencing technology, the species difference within these cultures and a specific SHH-blocking antibody, a set of genes was identified

that is stroma-derived and affects the extracellular space indirectly by remodeling the surrounding microenvironment to potentially promote tumor progression. Knowledge on these genes could potentially provide therapeutic targets in addition to SMO, but might also provide us with more insight into the roles of SHH in other biological systems.

It is important to note that the SHH-responsive genes found in our cocultures did not completely overlap with those found in fibroblasts stimulated with SHH ligand in the absence of tumor cells. We have assessed the expression of 6 of the coculture-derived target genes of SHH in ligand-treated monocultures and found that 4 of these were upregulated by SHH, whereas 2 were not. This suggests that approximately 30% of the genes we identified in the initial mRNA-Seq screen rely on the input of at least several tumor-derived signals besides SHH, and would not have been found in a ligand-treated monoculture.

Several of the factors identified in our *in vitro* coculture system were found to be strongly tumor-associated in two independent microarray datasets of pancreatic cancer. High

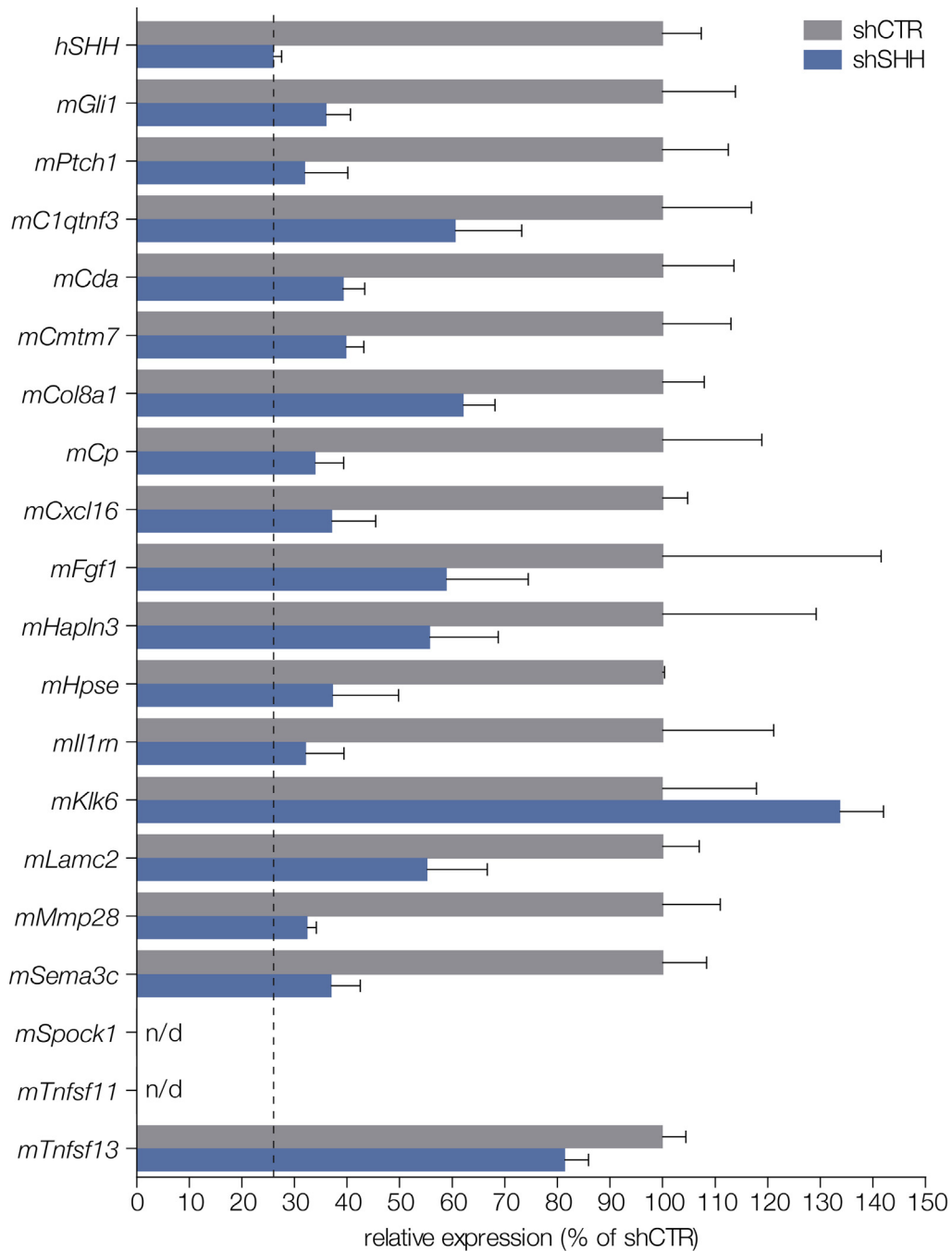


**Figure 5** – *In vitro* validation of targets in Capan-2 3D coculture. Capan-2 cells that were either stably transduced with a scrambled control (shCTR), or a SHH-targeting shRNA (shSHH) were cocultured with C3H10T1/2 fibroblasts as for Figure 1, and after 5 d, RNA was isolated and species specific qRT-PCR was performed for genes randomly selected from the GSEA analysis. Expression of the genes in the scrambled control cocultures was set to 100%. Shown is mean  $\pm$  SEM,  $n \geq 3$ .

expression of the HH-dependent stromal targets CDA, EDIL3, ITGB4, PLAUR and SPOCK1 were associated with poor prognosis in these patients, and most were found to be expressed in the stroma of human PDAC by immunohistochemistry. This makes them interesting molecules for further investigation. In light of the nucleoside analog gemcitabine being the most commonly used chemotherapeutic in pancreatic cancer patients, our finding of cytidine deaminase (CDA) expression as a predictor for patient outcome is interesting, as CDA is

known to catabolize gemcitabine to an inactive metabolite, and therefore patients with high expression of this gene would be less sensitive to the standard of care treatment regimen (Eda et al., 1998). The observed synergistic effect of Hedgehog inhibitors together with gemcitabine in several pre-clinical models of PDAC could be partially mediated by decreasing CDA expression in the stroma, resulting in increased availability of gemcitabine to reach and act on the tumor cells (Olive et al., 2009).

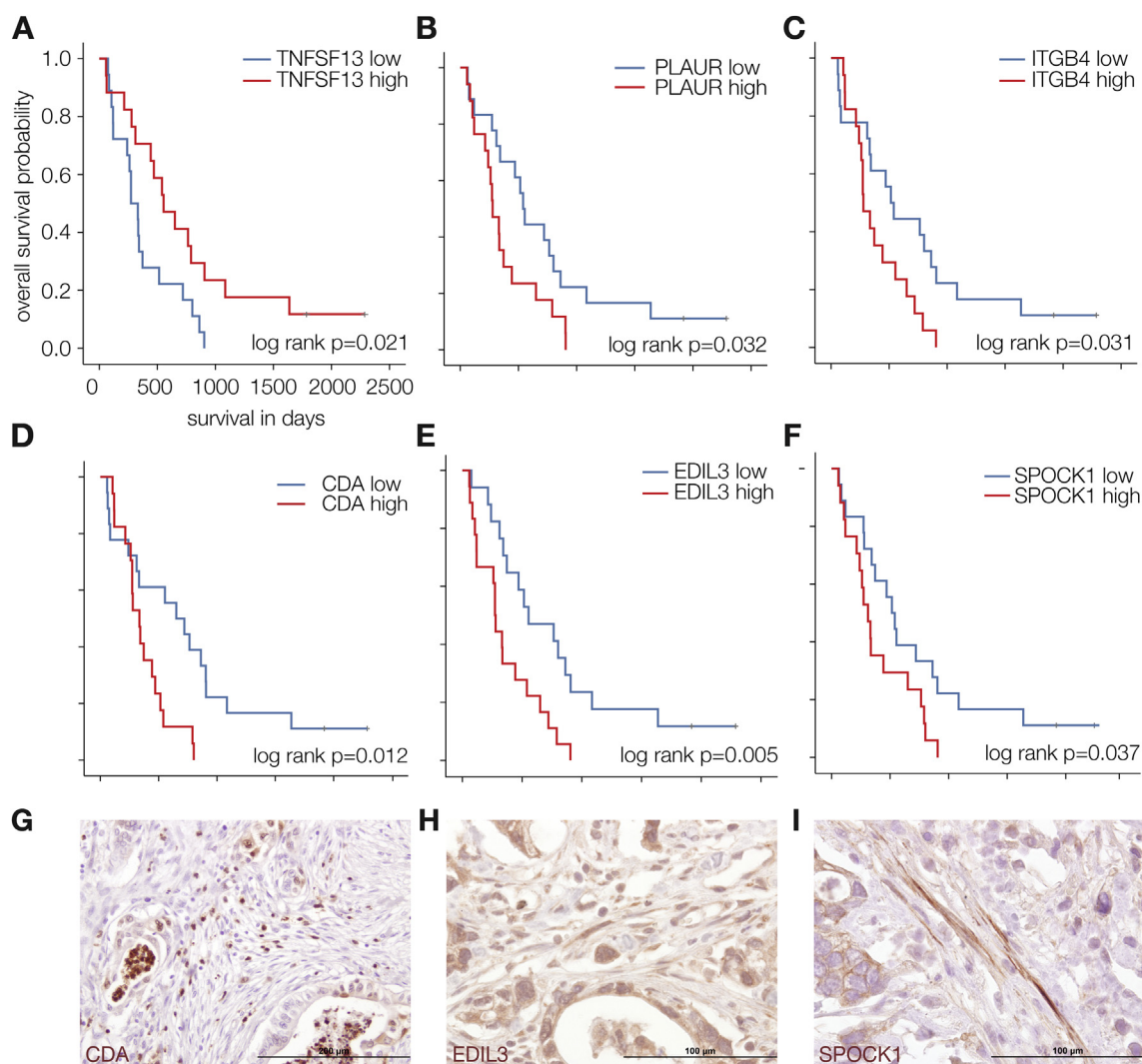


**Figure 6** – Stromal target genes identified in coculture correlate with survival in PDAC patients. A–F, Kaplan–Meier survival analysis of expression levels of individual genes from the 35 gene list. The median values of all 36 cases was defined as the expression cutoff separating patient tumors in high expression (red) vs. low expression group (blue). Shown are the Kaplan–Meier plots of the genes significantly associated with overall survival, as determined by log-rank test. G–I, immunohistochemistry for the indicated proteins was performed on tumor sections from patients from an independent cohort.

EGF-like repeats and discoidin I-like domains 3 (EDIL3, also known as DEL1) is an integrin ligand and plays an important role in mediating angiogenesis by preventing apoptosis and promoting adhesion of endothelial cells through interaction with  $\alpha v/\beta 3$  integrin receptor (Wang et al., 2012). This protein was also found to be overexpressed in hepatocellular carcinoma patients and high expression resulted in poor prognosis in this patient cohort (Sun et al., 2010). Additionally, it was shown that EDIL3 over-expression resulted in accelerated tumor growth in a transplantation model for osteosarcoma and lung carcinoma showing its strong potential as a tumor-promoting factor potentially by influencing the tumor vasculature (Aoka et al., 2002). Although a role for EDIL3 in PDAC has not been described before, our findings propose a similar tumor-promoting role in this disease.

The laminin receptor integrin beta 4 (ITGB4) is found up-regulated in tumor blood vessels as well as tumor cells in several

malignancies, where it has been shown to promote the invasive phase of tumor angiogenesis and enhance signaling function of multiple tyrosine kinases, including ErbB2, Met and EGFR (Giancotti, 2007). These findings make it an attractive target for cancer and anti-angiogenic therapy. Several studies in pancreatic cancer have shown upregulation of ITGB4 during tumor progression, but in these studies the tumor epithelium was found to be the main source of expression rather than the stroma, and this was confirmed by our stainings (Cruz-Monserrate et al., 2007).

Only very little information is available on the function of the proteoglycan SPOCK1 (testican-1). It has been implicated in regeneration of axons after brain injury and has been reported to be overexpressed in prostate cancer and HCC where it was shown to promote cell invasiveness and metastasis (Li et al., 2013). The physiological role of SPOCK1 remains largely unknown and this factor has not been investigated in the context of pancreatic cancer.

One of the best-studied molecules we identified in our coculture system and being associated with poor prognosis is the plasminogen activator, urokinase receptor PLAU. Previous studies already established this molecule to be over-expressed in pancreatic cancer patients and its association with worse outcome (Xue et al., 2008). Furthermore, stromal-derived PLAU expression was implicated in promoting pancreatic cancer metastasis via activation of uPA-plasminogen-MMP2 cascade and blockage of PLAU with a monoclonal antibody significantly decrease pancreatic tumor growth and liver metastasis in an orthotopic xenograft model of PDAC, making this molecule a prime target for therapy in patients (He et al., 2007). We were, however, not capable of showing expression of this protein in tissue from PDAC patients.

In conclusion, we provide a comprehensive, transcriptome-wide study to elucidate the factors regulated in the stromal compartment mediated by tumor cell-derived HH ligands. Aided by novel assays adapted from developmental biology, various gene expression analysis tools, and an extensive validation effort, we have managed to condense this transcriptome-wide data into a practical panel of interesting and relevant targets. Looking further into the mechanisms of how these stromal factors can influence the tumor compartment and the surrounding microenvironment, for instance by functional experiments in animals and immunohistochemical analyses of a large number of patient samples, should not only give more insight into the remarkable biology of pancreatic cancer, but hopefully push some of these proteins forwards as diagnostic tools or even therapeutic intervention targets.

## 5. Funding

This work was supported by NIH grant R01GM097035 to HR, a KWF Dutch Cancer Society Fellowship (UVA 2010-4813) as well as a KWF Dutch Cancer Society Research Grant (UVA 2012-5607) for MFB. These funding agencies had no involvement in study design or the decision to submit the article for publication.

## Appendix A. Supplementary data

Supplementary data related to this article can be found at <http://dx.doi.org/10.1016/j.molonc.2013.08.004>.

## REFERENCES

- Aoka, Y., Johnson, F.L., Penta, K., Hirata Ki, K., Hidai, C., Schatzman, R., Varner, J.A., Quertermous, T., 2002. The embryonic angiogenic factor Del1 accelerates tumor growth by enhancing vascular formation. *Microvasc. Res.* 64, 148–161.
- Badea, L., Herlea, V., Dima, S.O., Dumitrascu, T., Popescu, I., 2008. Combined gene expression analysis of whole-tissue and microdissected pancreatic ductal adenocarcinoma identifies genes specifically overexpressed in tumor epithelia. *Hepatogastroenterology* 55, 2016–2027.
- Bailey, J.M., Swanson, B.J., Hamada, T., Eggers, J.P., Singh, P.K., Caffery, T., Ouellette, M.M., Hollingsworth, M.A., 2008. Sonic hedgehog promotes desmoplasia in pancreatic cancer. *Clin. Cancer Res.* 14, 5995–6004.
- Berman, D.M., Karhadkar, S.S., Maitra, A., Montes De Oca, R., Gerstenblith, M.R., Briggs, K., Parker, A.R., Shimada, Y., Eshleman, J.R., Watkins, D.N., Beachy, P.A., 2003. Widespread requirement for Hedgehog ligand stimulation in growth of digestive tract tumours. *Nature* 425, 846–851.
- Bijlsma, M.F., Spek, C.A., Peppelenbosch, M.P., 2004. Hedgehog: an unusual signal transducer. *Bioessays* 26, 387–394.
- Burris 3rd, H.A., Moore, M.J., Andersen, J., Green, M.R., Rothenberg, M.L., Modiano, M.R., Cripps, M.C., Portenoy, R.K., Storniolo, A.M., Tarassoff, P., Nelson, R., Dorr, F.A., Stephens, C.D., Von Hoff, D.D., 1997. Improvements in survival and clinical benefit with gemcitabine as first-line therapy for patients with advanced pancreas cancer: a randomized trial. *J. Clin. Oncol.* 15, 2403–2413.
- Cruz-Monserrate, Z., Qiu, S., Evers, B.M., O'Connor, K.L., 2007. Upregulation and redistribution of integrin alpha6beta4 expression occurs at an early stage in pancreatic adenocarcinoma progression. *Mod. Pathol.* 20, 656–667.
- Eda, H., Ura, M., K.F.O., Tanaka, Y., Miwa, M., Ishitsuka, H., 1998. The antiproliferative activity of DMDC is modulated by inhibition of cytidine deaminase. *Cancer Res.* 58, 1165–1169.
- Ericson, J., Morton, S., Kawakami, A., Roelink, H., Jessell, T.M., 1996. Two critical periods of Sonic Hedgehog signaling required for the specification of motor neuron identity. *Cell* 87, 661–673.
- Erkan, M., Hausmann, S., Michalski, C.W., Fingerle, A.A., Dobritz, M., Kleeff, J., Friess, H., 2012. The role of stroma in pancreatic cancer: diagnostic and therapeutic implications. *Nat. Rev. Gastroenterol. Hepatol.* 9, 454–467.
- Giancotti, F.G., 2007. Targeting integrin beta4 for cancer and anti-angiogenic therapy. *Trends Pharmacol. Sci.* 28, 506–511.
- He, Y., Liu, X.D., Chen, Z.Y., Zhu, J., Xiong, Y., Li, K., Dong, J.H., Li, X., 2007. Interaction between cancer cells and stromal fibroblasts is required for activation of the uPAR-uPA-MMP-2 cascade in pancreatic cancer metastasis. *Clin. Cancer Res.* 13, 3115–3124.
- Hulsen, T., de Vlieg, J., Alkema, W., 2008. BioVenn – a web application for the comparison and visualization of biological lists using area-proportional Venn diagrams. *BMC Genomics* 9, 488.
- Li, Y., Chen, L., Chan, T.H., Liu, M., Kong, K.L., Qiu, J.L., Yuan, Y.F., Guan, X.Y., 2013. SPOCK1 is regulated by CHD1L and blocks apoptosis and promotes HCC cell invasiveness and metastasis in mice. *Gastroenterology* 144, 179–191e174.
- Mahadevan, D., Von Hoff, D.D., 2007. Tumor-stroma interactions in pancreatic ductal adenocarcinoma. *Mol. Cancer Ther.* 6, 1186–1197.
- Mortazavi, A., Williams, B.A., McCue, K., Schaeffer, L., Wold, B., 2008. Mapping and quantifying mammalian transcriptomes by RNA-Seq. *Nat. Methods* 5, 621–628.
- Neesse, A., Michl, P., Frese, K.K., Feig, C., Cook, N., Jacobetz, M.A., Lolkema, M.P., Buchholz, M., Olive, K.P., Gress, T.M., Tuveson, D.A., 2011. Stromal biology and therapy in pancreatic cancer. *Gut* 60, 861–868.
- Olive, K.P., Jacobetz, M.A., Davidson, C.J., Gopinathan, A., McIntyre, D., Honess, D., Madhu, B., Goldberg, M.A., Caldwell, M.E., Allard, D., Frese, K.K., Denicola, G., Feig, C., Combs, C., Winter, S.P., Ireland-Zecchini, H., Reichelt, S., Howat, W.J., Chang, A., Dhara, M., Wang, L., Ruckert, F., Grutzmann, R., Pilarsky, C., Izeradjene, K., Hingorani, S.R., Huang, P., Davies, S.E., Plunkett, W., Egorin, M., Hruban, R.H., Whitebread, N., McGovern, K., Adams, J., Iacobuzio-Donahue, C., Griffiths, J., Tuveson, D.A., 2009. Inhibition of Hedgehog signaling enhances delivery of

- chemotherapy in a mouse model of pancreatic cancer. *Science* 324, 1457–1461.
- Pei, H., Li, L., Fridley, B.L., Jenkins, G.D., Kalari, K.R., Lingle, W., Petersen, G., Lou, Z., Wang, L., 2009. FKBP51 affects cancer cell response to chemotherapy by negatively regulating Akt. *Cancer Cell* 16, 259–266.
- Planelles, L., Medema, J.P., Hahne, M., Hardenberg, G., 2008. The expanding role of APRIL in cancer and immunity. *Curr. Mol. Med.* 8, 829–844.
- Sinha, S., Chen, J.K., 2006. Purmorphamine activates the Hedgehog pathway by targeting Smoothened. *Nat. Chem. Biol.* 2, 29–30.
- Somasekaram, A., Jarmuz, A., How, A., Scott, J., Navaratnam, N., 1999. Intracellular localization of human cytidine deaminase. Identification of a functional nuclear localization signal. *J. Biol. Chem.* 274, 28405–28412.
- Subramanian, A., Tamayo, P., Mootha, V.K., Mukherjee, S., Ebert, B.L., Gillette, M.A., Paulovich, A., Pomeroy, S.L., Golub, T.R., Lander, E.S., Mesirov, J.P., 2005. Gene set enrichment analysis: a knowledge-based approach for interpreting genome-wide expression profiles. *Proc. Natl. Acad. Sci. U S A* 102, 15545–15550.
- Sun, J.C., Liang, X.T., Pan, K., Wang, H., Zhao, J.J., Li, J.J., Ma, H.Q., Chen, Y.B., Xia, J.C., 2010. High expression level of EDIL3 in HCC predicts poor prognosis of HCC patients. *World J. Gastroenterol.* 16, 4611–4615.
- Taipale, J., Chen, J.K., Cooper, M.K., Wang, B., Mann, R.K., Milenkovic, L., Scott, M.P., Beachy, P.A., 2000. Effects of oncogenic mutations in smoothed and patched can be reversed by cyclopamine. *Nature* 406, 1005–1009.
- Teglund, S., Toftgard, R., 2010. Hedgehog beyond medulloblastoma and basal cell carcinoma. *Biochim. Biophys. Acta.* 1805, 181–208.
- Thayer, S.P., di Magliano, M.P., Heiser, P.W., Nielsen, C.M., Roberts, D.J., Lauwers, G.Y., Qi, Y.P., Gysin, S., Fernandez-del Castillo, C., Yajnik, V., Antoniu, B., McMahon, M., Warshaw, A.L., Hebrok, M., 2003. Hedgehog is an early and late mediator of pancreatic cancer tumorigenesis. *Nature* 425, 851–856.
- Vincent, A., Herman, J., Schulick, R., Hruban, R.H., Goggins, M., 2011. Pancreatic cancer. *Lancet* 378, 607–620.
- Wang, Z., Kundu, R.K., Longaker, M.T., Quertermous, T., Yang, G.P., 2012. The angiogenic factor Del1 prevents apoptosis of endothelial cells through integrin binding. *Surgery* 151, 296–305.
- Wichterle, H., Lieberam, I., Porter, J.A., Jessell, T.M., 2002. Directed differentiation of embryonic stem cells into motor neurons. *Cell* 110, 385–397.
- Xue, A., Scarlett, C.J., Jackson, C.J., Allen, B.J., Smith, R.C., 2008 March. Prognostic significance of growth factors and the urokinase-type plasminogen activator system in pancreatic ductal adenocarcinoma. *Pancreas* 36 (2), 160–167.
- Yauch, R.L., Gould, S.E., Scales, S.J., Tang, T., Tian, H., Ahn, C.P., Marshall, D., Fu, L., Januario, T., Kallop, D., Nannini-Pepe, M., Kotkow, K., Marsters, J.C., Rubin, L.L., de Sauvage, F.J., 2008. A paracrine requirement for hedgehog signalling in cancer. *Nature* 455, 406–410.